JOURNAL OF THERMOPHYSICS AND HEAT TRANSFER
Vol. 22, No. 4, October–December 2008

Critical Discharge in Actively Cooled Wing Leading Edge of a Reentry Vehicle

L. Mongibello*
Ente per le Nuove Tecnologie l'Energia e l'Ambiente, Centro Ricerche Casaccia, 00123 Rome, Italy
and
L. de Luca†
University of Naples "Federico II," 80125 Naples, Italy

DOI: 10.2514/1.33824

The study of an innovative active cooling system of a wing leading edge of a hypersonic reentry vehicle making use of water is addressed. In particular, a steady model is developed to study the critical discharge of the cooling water into a very low-pressure ambient simulating the outlet conditions for both the reentry and wind-tunnel environments. Because of the strongly subcooled operating conditions, the model predicts no flashing within the duct connecting the outlet (hot) manifold to the vacuum ambient. The mass flow rate needed to remove the aerodynamic heat load acting on the external surface is calculated by an iterative procedure. At each iteration, for a fixed value of the mass flow rate, the pressure within the outlet manifold is calculated and the exit section critical pressure is determined as well. Subsequently, a detailed thermo-fluid-dynamic analysis is conducted to evaluate the head losses within the pipes and the peak wet wall temperature. The iteration stops when the mass flow rate guarantees no-boiling conditions throughout the system. The findings arising from the steady model are confirmed by unsteady numerical simulations of the system startup.

Nomenclature

D	=	contraction upper diameter of the outlet duct
d	=	outlet duct diameter
d_p	=	pipe diameter
e	=	pipe roughness
f	=	friction factor
G_c	=	critical flow rate per unit area
H	=	thermodynamic enthalpy
h	=	convective heat transfer coefficient
K	=	contraction coefficient
L	=	outlet duct length
L_p	=	pipe length
$\dot{m}$	=	mass flow rate
N	=	empirical parameter
Nu	=	Nusselt number
P	=	pressure
P_c	=	critical pressure
P_0	=	water stagnation pressure
P_{sat}	=	saturation pressure
Pr	=	Prandtl number
$\dot{Q}$	=	total aerodynamic heat rate
$\dot{q}_{\text{II}}$	=	aerodynamic heat flux
$\dot{q}'$, $\dot{q}'_{\text{II}}$	=	heat flux acting on pipe surface
Re	=	Reynolds number
S_e	=	external surface
S_p	=	pipe surface
T_0	=	water stagnation temperature (hot manifold)
T_b	=	water bulk temperature
T_{in}	=	inlet manifold temperature
T_w	=	wet wall temperature
$\bar{V}$	=	average velocity
v_g	=	vapor specific volume
v_l	=	liquid specific volume
x	=	streamwise spatial coordinate along the duct
x_E	=	equilibrium quality of the mixture
ζ	=	resistance factor
η	=	critical pressure ratio $\eta = P_c/P_0$
ν	=	kinematic viscosity
ρ_0	=	water stagnation density

I. Introduction

THE design and the development of technologies which operate in the aerothermodynamic environment of a typical reentry condition are one of the most demanding issues for the next generation of reentry vehicles. Within this context, the Italian Space Agency (ASI) is currently financing a space research project, named Advanced Structural Assembly (ASA), for the design, construction, and testing of a space wing involving new high-temperature materials.

Among the various technologies involved in the ASA program, one of the most innovative is the "active" cooling by means of water of the wing leading edge of a hypersonic reentry vehicle, as opposed to the ultra-high-temperature ceramics one. Indeed, the active cooled wing leading edge (ACWLE) is presently being designed and developed (by Thales Alenia Space) and will be eventually validated by means of tests to be conducted in the plasma wind tunnel SCIROCCO of CIRA (Italian Center for Aerospace Research). The contribution of the University of Naples "Federico II," Department of Energetics, Applied Thermodynamics, and Environment Control, now Department of Aerospace Engineering, lies in the field of the ACWLE activities which include, in particular, simulations of the steady closed-loop configuration of the cooling system and of the transient outlet phenomena in nearly vacuum conditions (i.e., both reentry and SCIROCCO environments) as well. On the other hand, Alenia Space has already carried out a first "cold" testing on a closed-loop hydraulic demonstrator [1], focusing on the experimental verification of the layout definition and on the validation of the analytical tools which will be used for the final design of the demonstrator to be subjected to the plasma wind-tunnel tests.

Presented at the AIAA SPACE 2007 Conference, Long Beach, CA, 18–20 September 2007; received 2 August 2007; revision received 19 May 2008; accepted for publication 20 May 2008.

*Researcher, Ph.D.
†Full Professor, Department of Aerospace Engineering; deluca@unina.it. AIAA Member.

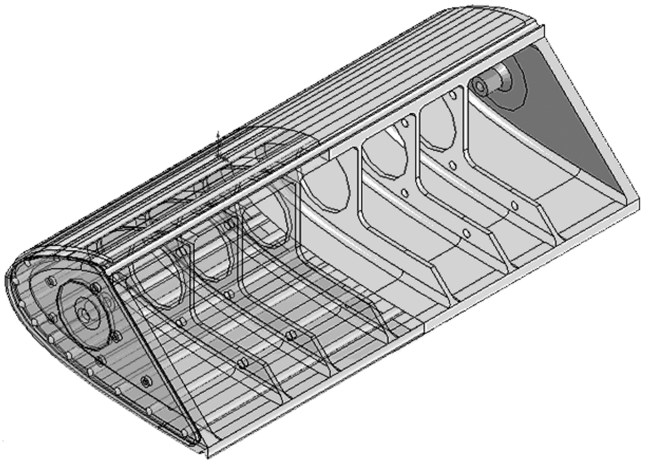

Fig. 1 ASA active cooling leading edge (courtesy of Alenia Space).

The reference mission profile and vehicle selected for the ASA project are derived from the Unmanned Space Vehicle Flying Test Bed experimental project, whose development is currently ongoing under CIRA responsibility. The mission profile applicable for the ASA purpose is an orbital reentry flight characterized by a 7.3 km/s entry velocity at a 120 km altitude and 0 deg entry angle.

The ACWLE body will be made of aluminum alloy. Pipes running all over the edge length (Fig. 1) will provide the coolant path necessary to remove the heat load acting on the external surface. Diameter and distances between pipe axes take into account the heat flux distribution foreseen during the test, and are determined by optimizing the cooling system capabilities. With reference to Fig. 1, the configuration presently under investigation considers 12 pipes with the same diameter ($d_p = 0.006$ m) and length ($L_p = 0.428$ m). Inlet (supply) and outlet (hot) manifolds will distribute and collect, respectively, water flowing into/from the pipelines located on the wing leading edge. The manifolds are geometrically symmetric due to the constant wing section, and are made of the same aluminium alloy as the wing profile. In the open configuration, the cooling water is discharged to the external ambient through an outlet duct followed by an end pipe (this last component not being shown in Fig. 1) of diameter $d = 0.008$ mm and length $L = 0.5$ m such that $L/d = 62.5$.

The present paper focuses on the open-loop configuration, for which the operating conditions refer to the discharge into an external ambient with a very low pressure level on the order of 100 Pa and a temperature of 20°C. Because of the sudden depressurization, the occurrence of flash evaporation phenomena could be expected. Flash evaporation, which typically occurs in the case of accidents to the cooling system of nuclear reactors, consists of a nonequilibrium change of phase from liquid to vapor and of an associated fall of the pressure caused by the expansion of the fluid. Indeed, when a liquid flows within a pipeline and is subjected to a sudden depressurization, it experiences nonequilibrium conditions, and evaporation abruptly occurs at a location where the pressure falls below the saturation one (pressure undershoot). In the flash evaporation, bubbles do not collapse (as they do in cavitation) and the system behaves as a mixture of liquid and bubbles traveling at high speed. An up-to-date review article, covering experimental as well as numerical aspects of such phenomena, is due to Pinhasi et al. [2].

Of course, in the case of the active cooling by means of water of the wing leading edge of a hypersonic reentry vehicle, the system should be properly designed so as to prevent flashing.

A previous theoretical analysis proved that, for the present system, the transient effects are limited to a few tenths of seconds, whereas the planned test runs in SCIROCCO will be on the order of 20 min. Thus, to calculate the critical flow rate and pressure ratio at the exit section, a steady-state model has been developed. Nevertheless, numerical simulations carried out by means of RELAP5-3D code,[‡] developed by Idaho National Engineering and Environmental Laboratory, will be presented as well, confirming the quick reaching of the steady state.

[‡]http://www.inel.gov/relap5, 2007.

II. Flashing Model

A. Flashing Phenomena

During a transient flashing phenomenon, occurring when a saturated or subcooled liquid in a pipeline is suddenly exposed to a very low-pressure boundary condition at its outlet section, typically two expansion waves move upstream of the pipeline. The first one is the (classic) rarefaction wave propagating at sound speed of the liquid phase, on the order of 1000 m/s, which conveys the information concerning the downstream very low pressure. In the area downstream of such a wave, pressure falls below the saturation pressure and settles up to the arrival of a second slow wave, whose velocity is on the order of 10 m/s, which represents the traveling boiling front and further lowers the pressure level. The pressure undershoot can be either simulated numerically, as done by Ivashnyov et al. [3], or predicted by means of semi-empirical correlations. Moreover, due to the increase of the flow velocity, caused by the expansion of the mixture after boiling, and the parallel decrease of the sound speed, sonic conditions are reached at the outflow section, namely, at the exit section where the flow is *choked*.

Besides the numerical simulation support, some physical considerations, also based on the literature survey, allowed us to consider that, for the present problem, the efflux may be studied essentially by a steady model. As a consequence, on one hand, a steady model has been developed (it is described in the next section) which allowed calculation of the (critical) flow rate and the pressure ratio at the exit section; on the other hand, the numerical analysis proved that the transient effects are limited to a few tenths of a second, whereas the planned test runs in SCIROCCO will be on the order of 20 min, thus confirming the steady assumption.

Within the papers specifically devoted to the numerical simulation of such a phenomenon (namely, unsteady one-dimensional two-phase flow), the most significant papers of the literature appear to be those of Nigmatulin and Soplenkov [4] and of Ivashnyov et al. [3]. The first one [4] is mainly devoted to the determination of the so-called pressure undershoot. However, due to the intrinsic difficulties arising in modeling such a complex nonequilibrium flow, one may refer to semi-empirical correlations, as reported by Pinhasi et al. [2].

A crucial, as well as difficult, problem is modeling the nonequilibrium boiling process. The model proposed by Nigmatulin and Soplenkov [4] is based on the assumption of a constant number of nucleation centers that predicts a pressure drop higher than that detected during experiments. In effect, this model does not take into account the continuous rupture of bubbles due to an instability of the Kelvin–Helmholtz kind. This last effect produces a more intense boiling and, as a consequence, an increase of the number of nucleation centers. The rupture of the bubbles occurs just within the region upstream of the slow expansion wave (not detected by the first, more classic model) and the related effect is the further lowering of the pressure (Ivashnyov et al. [3]).

Other interesting papers regarding the modeling of the sudden depressurization of pipelines are due to Fairuzov [5], Hahne and Barthau [6], Pinhasi et al. [7], and Duan et al. [8].

In this work, the numerical simulations of the sudden unsteady outflow in a vacuum of the cooling water have been carried out by means of RELAP5-3D code,[‡] specifically developed to simulate crash events in the refrigeration system of nuclear reactors by Idaho National Engineering and Environmental Laboratory.

B. Steady Model of the Critical Discharge

A very large amount of papers are available in the specialized literature concerned with the steady discharge of a two-phase flow subjected to a sudden deep depressurization at the exit section of a pipeline. A consistent bulk of such contributions, proposing algebraic as well as more complicated differential models, is reported in the reference list of the present paper [9–14].

In this work, the model proposed first by Henry [9] and Henry and Fauske [10] has basically been adopted and developed for calculations. It has to be stressed that applying such a model requires the localization of the flashing inception, which is a critical matter depending on the nucleation site and growth of the vapor bubbles. However, for the present conditions, due to the very high degree of subcooling and the fully developed turbulent regime (the pipe is relatively long, namely $L/d = 62.5$, and as will be seen, the Reynolds number is on the order of 10^5), one may assume that the discharge is critical (i.e., the mass flow rate exhibits a maximum with respect to the throat pressure) and, more important, that flashing occurs just at the exit section. The present assumption follows the arguments developed by Fraser and Abdelmessih [11,12], who report results of a modeling and experimental study of the critical two-phase flow of saturated and subcooled water through long tubes (i.e., friction dominated). In particular, they accurately control the location of the flashing inception through the use of a properly designed device.

Fraser and Abdelmessih [11,12] have shown that the exit pressure does indeed approach saturation for highly subcooled stagnation states, that is, when flashing inception occurs at the exit with a negligible superheat. In more details, they show that, depending on the location of the flashing inception, the critical mass flux may range within a minimum and a maximum value. However, for highly subcooled stagnation states, this range tends to vanish and one may assume that flashing occurs at the exit where pressure is approximately equal to the saturation one.

Indeed, one might also suspect that flashing occurs downstream of the exit section, as discussed by Simões-Moreira and Bullard [13]. These authors argue that two different regimes may establish in the critical discharge of a highly subcooled liquid. The former, where the nucleation starts within the nozzle, either at the wall or at any other nucleation site in the bulk of the liquid, but the bubble growth rate is rather fast and the flow issues from the nozzle as a two-phase mixture, which then expands into the low-pressure ambient; the latter, where the evaporation takes place downstream of the exit plane at the surface of an evaporating metastable liquid jet (defining a liquid core surrounded by a cone of evaporation), which remains more or less undisturbed. The first regime is more likely to occur in long tubes ($L/d > 5$), where friction plays a larger role. The other one, on the contrary, is more likely to occur in metastable liquid evaporation at a high degree of metastability and in short orifice nozzles.

From the preceding discussion it is clearly evident that, for the problem presently under study, the hypothesis that the flow issues from the duct as a two-phase mixture just at the exit section is firmly valid. By assuming homogeneous flow (no slip condition between liquid and vapor phases, which is valid for low-quality or high-pressure cases), nonequilibrium thermodynamic processes, incompressible liquid phase, a simplified formula for the evaluation of the critical flow rate per unit area, or critical mass flux G_c is given by [9]

$$G_c^2 = -\left[(v_g - v_l)N\frac{\mathrm{d}x_E}{\mathrm{d}P}\right]_t^{-1} \tag{1}$$

where v_g and v_l are the vapor phase specific volume and the liquid phase specific volume, respectively, N is an empirical parameter, P is the pressure, and x_E is the equilibrium quality of the mixture. The subscript t indicates that all the enclosed quantities are evaluated at the throat, that is to say, at the choking section and equilibrium conditions corresponding to the (unknown) critical exit pressure. According to Henry [9] and Fraser and Abdelmessih [12], due to the very low quality, here, N is taken equal to 20 x_E, moreover, the derivative $\mathrm{d}x_E/\mathrm{d}P$ is evaluated by interpolating with the spline technique the water properties tables from 2005 ASHRAE Handbook.[§]

Because of the strong subcooled conditions that characterize the system under consideration, another more simplified model (Celata et al. [14]) may be used as a reference, which assumes that the pressure at the pipe exit section coincides with the saturation one:

$$G_c = \sqrt{\frac{2[P_0 - P_{\mathrm{sat}}(T_0)]}{v_l(1 + K + fL/d)}} \tag{2}$$

which basically appears as a modified Bernoulli equation, including localized losses due to entrance effects and distributed losses due to friction along the pipeline. K is the inlet contraction coefficient, f is the friction factor, and P_0 and T_0 are the stagnation pressure and temperature, respectively.

As already found by Fraser and Abdelmessih [11,12], it will be shown hereafter that Henry's [9] and Celata et al.'s [14] models practically coincide in the field of the actual operating conditions.

In Henry's model [9], the critical pressure may be evaluated by combining the critical flow rate of Eq. (1) with the relationship for the pressure drop along the pipe (Lenclud and Venart [15], Ould Didi et al. [16], Wongwises and Suchatawut [17], Yoon et al. [18]):

$$\eta = 1 - \left(1 + K + f\frac{L}{d}\right)\frac{G_c^2 v_l}{2P_0} \tag{3}$$

η being the critical pressure ratio, that is, $\eta = P_c/P_0$.

The coefficient K, relative to the entrance head losses, has been evaluated by means of the semi-empirical formula given by White [19]:

$$K = 0.42\left(1 - \frac{d^2}{D^2}\right) \tag{4}$$

where D is the contraction upper diameter of the outlet duct.

The friction coefficient f accounts for the distributed head losses along the duct and has been evaluated for turbulent flow by means of the explicit formula proposed by Haaland [20]:

$$\frac{1}{\sqrt{f}} = -1.8\log_{10}\left(\frac{6.9}{Re} + \left(\frac{1}{3.7}\frac{e}{d}\right)^{1.11}\right) \tag{5}$$

where Re is the Reynolds number and e/d is the pipe relative roughness.

Equations (1) and (3) constitute a transcendental system for the critical mass flux and the pressure ratio, which allows the simultaneous determination of both the quantities and requires only a knowledge of the upstream stagnation conditions as well as the geometry of the pipe. The solution is found iteratively by adjusting the pressure ratio until both equations are satisfied.

However, as will be seen in the following part of the paper, for the present application, the critical mass flux has to be considered as a known quantity, and the stagnation pressure (namely, the pressure within the hot outlet manifold) considered as an unknown one, accordingly.

III. Results

A. Heat Transfer Modeling

The distribution of the aerodynamic heat flux on the wing surface has been calculated numerically at CIRA for the actually designed profile mission, and represents, together with the water temperature at the inflow of the inlet manifold, $T_{\mathrm{in}} = 20°\mathrm{C}$, a given data. The external heat flux is considered constant along the spanwise direction of the wing, and its variation along the wing profile has been reconstructed employing at each point of the profile the maximum value calculated during the entire reentry duration. Of course, this position leads one to overestimate by several percent the critical mass flow rate needed to remove the aerodynamic heating.

Figure 2, showing a portion of the wing section, is helpful to understand the approximation adopted to transfer the aerodynamic heat flux acting on the external surface to the pipes surface. With reference to the energy (per unit width) balance relative to sector II, $\dot{q}_{\mathrm{II}}$ represents the average aerodynamic heat flux acting on the external surface S_e, whereas $\dot{q}'_{\mathrm{II}}$ is the actual heat flux entering the pipe surface S_p, which is supposed to be equally distributed along the surface. The surfaces AD and BC are considered adiabatic, laying midway between the centers of the adjacent sectors. The surface CD

[§]http://www.ashrae.org.

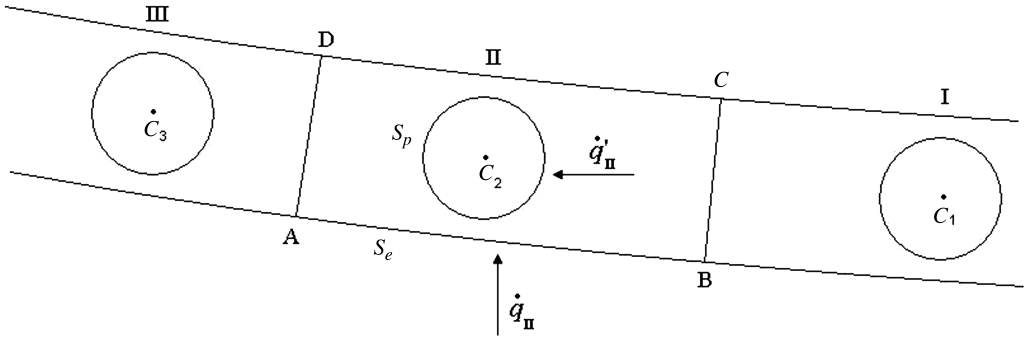

Fig. 2 Sketch of a portion of the wing section.

is adiabatic too, because the internal radiative and conductive heat fluxes are considered practically negligible. Therefore, assuming that the external aerodynamic heat is totally absorbed by the pipelines, the energy balance yields

$$\dot{q}_{II} S_e = \dot{q}'_{II} S_p \tag{6}$$

Equation (6) is used to calculate the heat fluxes entering the pipes' surfaces. The results are showed in Table 1.

To the aim of calculating the minimum critical mass flow rate that guarantees no-boiling conditions of water inside the whole cooling system, an iterative approach has been adopted. At each iteration, for each guess, mass flow rate $\dot{m}$, a simple global energy balance applied from inlet to outlet manifolds, $\dot{m}\Delta H = \dot{Q}$ (H being the thermodynamic enthalpy and $\dot{Q}$ the total aerodynamic heat rate), yields the bulk water temperature in the outlet manifold T_0 and the saturation pressure $P_{sat}(T_0)$ as well. By means of Henry's flashing model [9], the guess mass flux being assumed as the critical one, the pressure within the outlet manifold P_0 is then calculated, and the critical pressure at the exit section of the outlet duct is determined as well. Subsequently, to verify that no-boiling conditions are satisfied within each upstream pipe, a detailed thermo-fluid-dynamic analysis is conducted so as to distribute the total mass flow rate among the 12 pipelines, to evaluate the relevant head losses, and to estimate the local wet wall temperatures. The calculation ends if the resulting maximum wall temperature is lower than the boiling one at P_0. Otherwise, a new iteration starts with the mass flow rate increased by a step of 0.01 kg/s. The initial condition of $\dot{m} = 0.25$ kg/s is assumed.

For the present configuration, the minimum "no-boiling" critical mass flow rate $\dot{m} = 0.47$ kg/s is found, which corresponds to a stagnation pressure in the outlet manifold P_0 equal to 105.620 kPa. The critical pressure at the outlet duct exit section P_c and the stagnation temperature T_0 at the outlet manifold are 6.447 kPa and 37.4°C, respectively. It has to be immediately stressed that, for this temperature, the saturation pressure is $P_{sat}(T_0) = 6.471$ kPa, nearly coincident with the critical one.

Table 1 Heat fluxes evaluation

Sector/pipe	Maximum averaged aerodynamic heat flux, W/m^2	Actual heat flux entering each pipe, W/m^2
1	250,491	309,633
2	269,214	494,166
3	306,208	497,092
4	385,064	522,964
5	434,884	486,805
6	401,981	407,322
7	344,030	324,874
8	289,568	281,126
9	219,140	270,880
10	151,156	252,601
11	125,980	250,629
12	119,576	152,249

The following sections will provide details about both Henry's model [9] application and the detailed thermo-fluid-dynamic analysis.

B. Henry's Model Application

The model has been initially tested (not shown herein) by comparing the numerical results to various experimental and numerical data of literature (Henry [9], Henry and Fauske [10], Fraser and Abdelmessih [11,12]), for both saturated and subcooling conditions. As expected, the effectiveness of the model is better for (strong) subcooling conditions. Then, calculations have been made for the problem under examination, that is, for $d = 8$ mm, $L/d = 62.5$, $e/d = 10^{-5}$, $T_0 = 37.4$°C, and various $P_0/P_{sat}(T_0)$ values.

Figure 3 reports the two plots of the nondimensional mass flux $G_c^2/[2\rho_0 P_{sat}(T_0)]$, ρ_0 being the water stagnation density, against $P_0/P_{sat}(T_0)$, as obtained by employing Henry's model [9] and Celata et al.'s model [14]. At low values of P_0/P_{sat}, the flow rate predicted by the two models differ from each other by about 5%, whereas they practically coincide starting from a unit pressure ratio.

As an overall remark, by entering the value of the mass flow rate into the diagrams shown in Fig. 3, one may draw the operating value of the ratio $P_0/P_{sat}(T_0)$ and, ultimately, the pressure in the outlet manifold. For the actually designed conditions, because the no-boiling constraint requires $\dot{m} = 0.47$ kg/s (see next section), that is, $G_c = 9350.4$ kg $\cdot$ s^{-1} $\cdot$ m^{-2}, the nondimensional critical flux results $G_c^2/[2\rho_0 P_{sat}(T_0)] = 6.78$ to which a pressure ratio $P_0/P_{sat}(T_0)$ of 16.33 corresponds. In conclusion, the system has to be designed such that the pressure inside the outlet (hot) manifold is 105.620 kPa.

It also has to be stressed that the duct Reynolds number is $\bar{V}d/\nu = 1.15 \cdot 10^5$, evaluated for an average velocity $\bar{V} = 9.43$ m/s

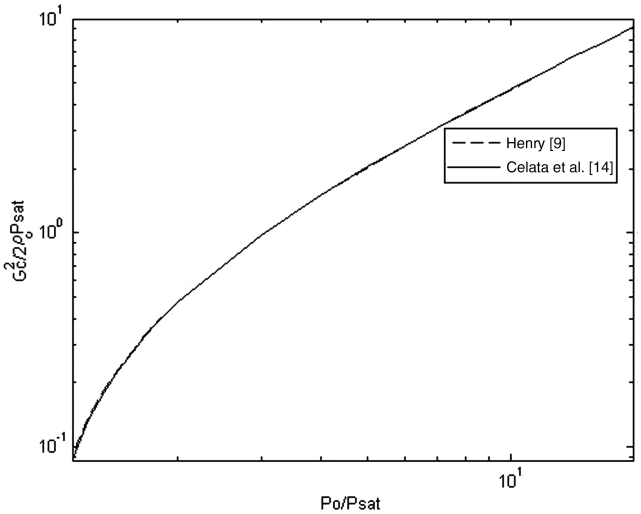

Fig. 3 Nondimensional critical mass flux as a function of the dimensionless stagnation pressure.

corresponding to the mass flow rate $\dot{m} = 0.47$ kg/s. Thus, for this Reynolds number and the relatively high $L/d = 62.5$, the flow within the outlet duct may be considered fully developed turbulent, as anticipated in Sec. II.B.

The previous results about the critical discharge have been confirmed by unsteady numerical simulations carried out by means of RELAP5-3D code (see ‡ footnote on p. 678) designed to simulate a wide variety of hydraulic and thermal transients involving mixtures of vapor, liquid, noncondensable gases, and nonvolatile solute. In addition to the hydrodynamic models for simulating homogeneous flows in thermal equilibrium, the code includes nonhomogeneous and nonequilibrium models for two-phase systems. From the numerical point of view, RELAP5-3D solves the system of field equations using either a semi-implicit or a nearly implicit finite difference technique on a staggered grid. That is, the mass and energy balance equations are written in nodes, whereas the momentum equations are written at junctions, which connect the nodes to each other.

With reference to the present investigation, the one-dimensional numerical simulation of the transient discharge of water from the hot manifold (stagnation chamber) to a nearly vacuum ambient through the outlet duct has been carried out by employing homogeneous and nonequilibrium models. As regards the numerical scheme, the semi-implicit scheme with Courant time-step control is selected due to its higher efficiency in rapid transient simulations. Figure 4 shows the nodalization scheme adopted for the actual system.

The computational domain consists of a time-dependent volume (TMDPVOL in Fig. 4, simulating the hot manifold) where stagnation conditions are set, a pipe component (the outlet duct) discretized in 100 volumes, and another time-dependent volume (simulating the external ambient and here representing the nearly vacuum conditions). Two junctions connect the hot manifold to the pipe and the pipe to the external ambient. The two TMDPVOLs are used to assign pressure and temperature boundary conditions, namely, for the present case, the hot manifold pressure is kept fixed at 105.620 kPa and temperature at 37.4°C, while the external ambient pressure is kept fixed and equal to 100 Pa and temperature equal to 20°C. The Henry and Fauske choking model [10] is turned on at the outlet junction and is used at each time step to control the occurrence of choking at the duct exit section. So, if the flow is choked, then the model works like a discharge boundary condition. The entrance and friction losses are congruent with those considered in the previously reported models. The maximum time step used is equal to 10^{-5} s, whereas the constant spatial step resulting from the pipe discretization is equal to 5 mm (the pipe is 500 mm long and contains 100 volumes). The employed initial conditions prescribe zero velocity, pressure equal to 105.620 kPa, and temperature equal to 37.4°C all along the pipe length. Thus, $P_0/P_{\text{sat}}(T_0)$ is taken equal to 16.33, and this pressure ratio is also the initial condition all over the system.

The relatively rapid attaining of the steady conditions is clearly evident from Fig. 5, where the time evolution of the dimensionless pressure $P_0/P_{\text{sat}}(T_0)$ at three typical locations x/L along the duct is reported. The steady conditions are clearly attained in all the locations here considered to within about three-tenths of a second. This is confirmed by the time trend of the mass flow rate, which is reported in Fig. 6. The result depicted by this last picture is very meaningful because it shows that the steady value of the flow rate is equal to 0.47 kg/s, that is, the very same value predicted by the steady-state model is uncovered to within a high accuracy.

With reference again to Fig. 5, note that the initial pressure drop, caused by the expansion wave traveling at sound speed, becomes weaker going back through the pipe. This decrease in the initial rate of depressurization is a result of the broadening of the rarefaction

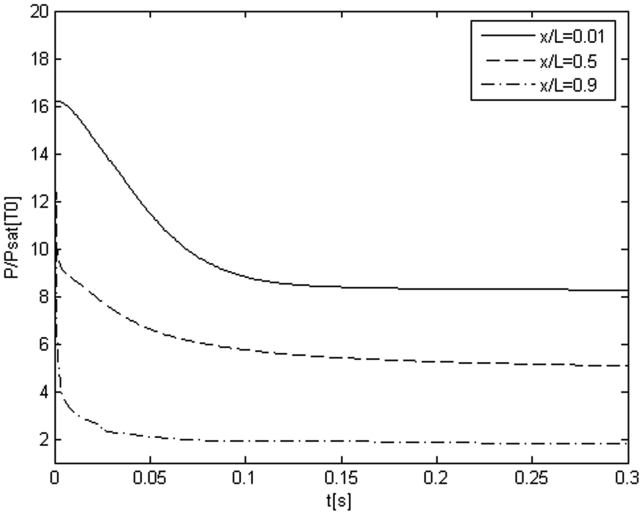

Fig. 5 Time evolution of the pressure while attaining the steady conditions.

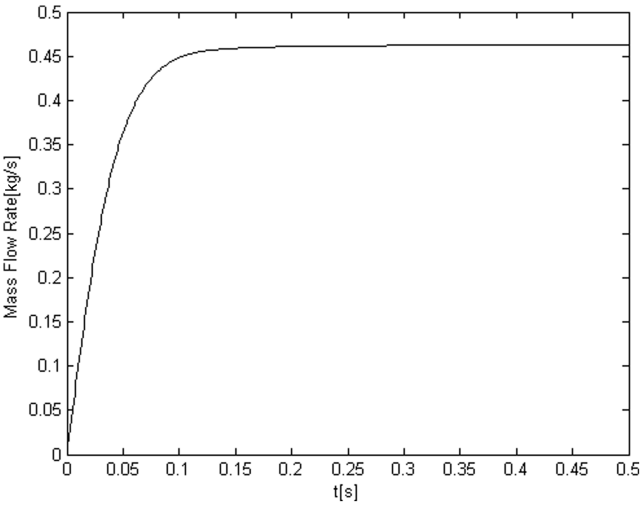

Fig. 6 Time variation of the mass flow rate.

wave, as evidenced in several numerical and experimental data reported by Ivashnyov et al. [3].

The steady values of the dimensionless pressure at the three stations reflect the streamwise pressure distribution due to inlet and distributed head losses, as shown next in Fig. 7. It has to be noticed that, due to the strong subcooled conditions of the system, water does not flash within the pipe and the pressure at the pipe exit, $x/L = 1$, practically equals the equilibrium saturation value $P_{\text{sat}}(T_0) = 6.471$ kPa.

Further numerical simulations have been performed, using up to 200 volumes for pipe discretization, as well as up to a time step of 10^{-6} s, without observing any substantial variation of results.

C. Thermo-Fluid-Dynamic Analysis

As stated in Sec. III.A, at each iteration, once the stagnation pressure has been calculated for a guess mass flow rate, a detailed thermo-fluid-dynamic analysis is carried out through the following two steps: numerical simulation of the local flowfield within the basic

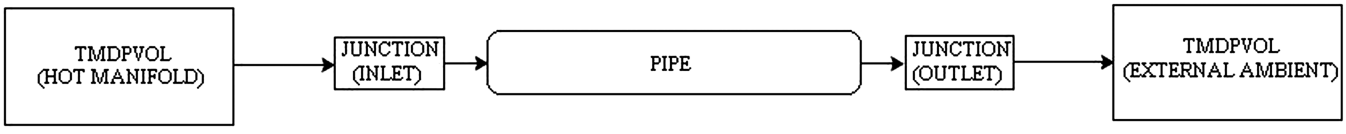

Fig. 4 Nodalization scheme.

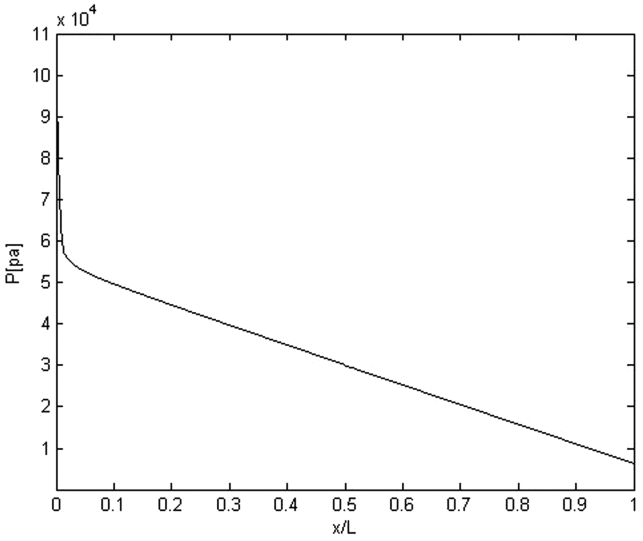

Fig. 7 Steady-state distribution of the pressure along the discharge duct.

components of the system (inlet manifold, pipes, outlet manifold, and duct) with the aim of computing the mass flow rate relative to each pipeline, and evaluation of the convective heat transfer coefficients to the pipelines to calculate the wet wall temperature field.

The FLUENT solver (release 6.3) has been used to simulate the steady 3-D turbulent flowfield within the whole system. The "standard k-ε" model has been implemented to accomplish the turbulence closure. Because of the complexity of the geometry under investigation, a hybrid mesh is used. Actually, the manifolds are discretized by means of tetrahedral cells, whereas hexahedral cells are used for the discretization of the inlet duct, the outlet one, and the 12 pipelines. Figures 8 and 9 are relative to the coarsest mesh and show the cell distribution around the inlet region (the outlet one is clearly similar) and along the pipelines. As can be partially seen, a bell-shaped axial distribution of the cells has been applied to the pipelines to reduce the computational cost of the simulations.

As regards the numerical schemes, the convective and diffusive terms are discretized by using the second-order upwind scheme, and the coupling between pressure and velocity is solved by means of the SIMPLE algorithm. As far as the boundary conditions are concerned, the mass flow rate is assigned at the inflow section of the inlet manifold, whereas the stagnation pressure resulting from the flashing model is assigned at the outflow section of the hot manifold.

Grid independence has been checked by monitoring the computed averaged pressure at the inflow section of the inlet manifold. For this purpose, six meshes ranging from 7×10^5 to 1.2×10^6 cells have been used. With reference to the minimum mass flow rate that guarantees no boiling throughout the system, that is, $\dot{m} = 0.47$ kg/s, the results indicated no sensible variation of such an averaged

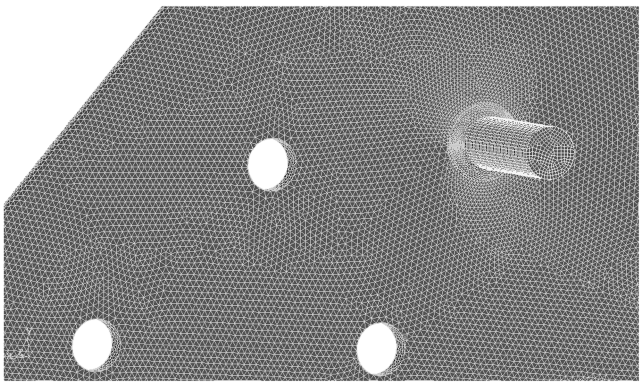

Fig. 8 Cell distribution on manifold and inlet duct.

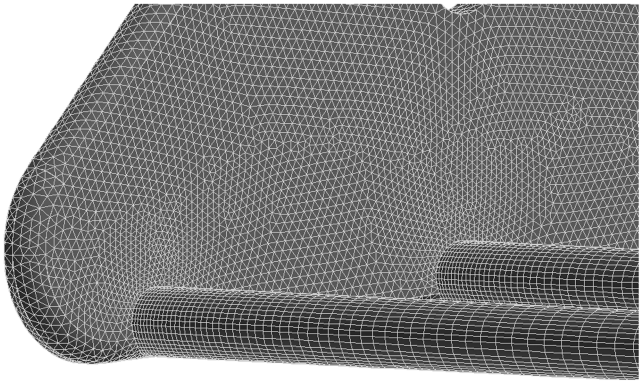

Fig. 9 Pipelines hexahedral mesh.

pressure in the range from 9×10^5 to 1.2×10^6 cells. In all cases, underrelaxation is used and the calculation convergence is achieved by imposing a maximum admissible residual of 10^{-6}.

Figures 10 and 11 refer to the preceding no-boiling case and show two sketches of the streamline distributions relative to the inlet and outlet manifold, respectively. Figure 11, in particular, shows the swirling motion of the water while flowing from the manifold toward the discharge duct.

As a main finding, the mass flow rate reaches its maximum value in the pipe where the actual heat flux is maximum; this last does not correspond to the peak of the external heating because it occurs in an area where the pipelines are rather far away from each other. The resulting mass flow rate distribution through each pipeline has been subsequently employed in the thermal analysis. Under the assumption of fully developed turbulent flow, for each pipe, the mean temperature (between inlet and exit sections), the Nusselt number, the convective heat transfer coefficient h, and, as a final step, the wet wall temperature at the exit section have been calculated within a cascade procedure. In particular, the Nusselt number has

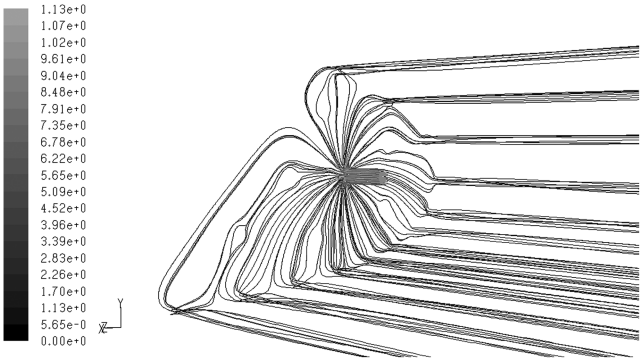

Fig. 10 Streamlines colored by velocity magnitude (m/s) in the inlet manifold.

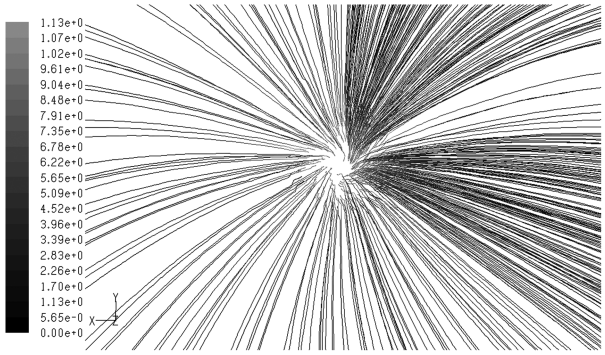

Fig. 11 Streamlines colored by velocity magnitude (m/s) in the outflow section of the hot manifold (inside view).

Table 2 Data relative to the minimum no-boiling mass flow rate

Pipe	Heat flux, W/m^2	Mass flow rate, kg/s	Outflow temperature, K	Mean (inlet/outlet) temperature, K	Re	Pr	$h(x = L_p)$, W · m^{-2} · K^{-1}	Wet wall temperature ($x = L_p$), K
1	309,633	0.03983	308	300.5	10,565	5.41	8229.2	345.63
2	494,166	0.04005	316.8	304.91	11,739	4.82	8764.3	373.2
3	497,092	0.04112	316.3	304.67	12,052	4.82	8974.5	371.72
4	522,964	0.04281	316.6	304.79	12,548	4.82	9304.5	372.78
5	486,805	0.04176	315.5	304.25	12,240	4.83	9099.8	368.99
6	407,322	0.03578	315	303.99	10,487	4.84	7914.5	366.44
7	324,874	0.03588	310.5	301.74	10,517	5.1	7934.6	351.42
8	281,126	0.03719	307.6	300.29	10,901	5.5	8197.1	341.88
9	270,880	0.03543	307.8	300.38	10,385	5.45	7844	342.29
10	252,601	0.03711	306.1	299.57	10,877	5.56	8181.2	337.01
11	250,629	0.04054	304.9	298.97	10,754	5.83	8362.9	334.90
12	152,249	0.04248	299.9	296.46	10,095	6.13	8164.8	318.56

been evaluated by means of the following equation (Baehr and Stephan [21]):

$$Nu = \frac{(\zeta/8)(Re - 1000)Pr}{1 + 12.7\sqrt{\zeta/8}(Pr^{2/3} - 1)}\left[1 + \left(\frac{d}{L}\right)^{2/3}\right] \tag{7}$$

where Pr is the Prandtl number and with the resistance factor given by

$$\zeta = \frac{1}{(0.79\,\ell_n\, Re - 1.64)^2} \tag{8}$$

For each pipe, the wet wall temperature at the exit section is given by $T_w = T_b + \dot{q}'/h$, where T_b is the water bulk temperature at the exit section, h is the local convective heat transfer coefficient, and $\dot{q}'$ is the local heat flux.

The values of the water properties have been based on the arithmetic mean of the inlet and outlet bulk temperatures. The sharp variation of the viscosity coefficient with temperature approaching the wall has been accounted for (Baehr and Stephan [21]).

Data relative to the minimum no-boiling mass flow rate ($\dot{m} = 0.47$ kg/s) are reported in Table 2. The head losses between outlet and inlet sections, as evaluated by FLUENT, are about 46.77 kPa. This allows one to estimate the inflow conditions in the supply manifold yielding the desired outflow conditions in the hot manifold. All of the calculated wet wall temperatures (that is to say, inside the pipe boundary layer) are found to be below the "equilibrium" boiling limit at the saturation pressure P_0.

This condition, together with the basic assumption that the external aerodynamic heating has been considered constant over the entire reentry duration (typically 1800 s) and kept equal to its maximum value, overestimates the needed mass flow rate and makes the design of the proposed thermal protection system very safe. On the other hand, from a practical point of view, one also has to consider that strictly applying the calculated mass flow rate for 1800 s means that more than 800 kg of water would be needed in the process. Even if one would reduce this value by a factor of 2 to take into account the overestimation of the thermal load, this mass could be not realistic from the technological point of view (storage tank and plumbing all require additional mass that must fly with the vehicle) and thus, ultimately, the proposed solution would appear more expensive as compared to traditional systems. On the contrary, the advantage of the active cooling system over the other systems lies in the reusability unique feature.

IV. Conclusions

A new active cooling system of a wing leading edge (ACWLE, currently being designed by Thales Alenia Space within the ASA space program of ASI) of a hypersonic reentry vehicle has been addressed. This innovative idea could be successful, as opposed to more or less conventional technologies, that is, among others, the one making use of ultra-high-temperature ceramics.

The mission profile has first been defined, together with the external aerodynamic heat load, followed by an overall thermo-fluid-dynamics analysis of the cooling system, yielding detailed information about the mass flow rate distribution of the coolant within the various pipelines of the system, the local convective heat transfer coefficients, and, finally, the fluid as well as wet wall temperatures. The basic design constraint is that the water mass flow rate must remove all the external heat, preserving no-boiling conditions all over the system.

In view of the open-loop operation in very low-pressure conditions (namely, both reentry and wind-tunnel environments), a study has been carried out to verify the possible occurrence of flashing phenomena due to the sudden exposure of the water to the nearly vacuum ambient. A steady theoretical model (based on Henry's model [9]) has been developed, and unsteady numerical simulations have been carried out as well.

Because of the strongly subcooled operating conditions and the flow in the outlet duct (connecting the outlet manifold to the vacuum ambient) being highly friction dominated (i.e., fully developed turbulent with $Re = 1.15 \times 10^5$), the steady model assumes a critical efflux (the exit section is chocked) and no flashing within the duct. Indeed, to the aim of calculating the minimum critical flow rate that guarantees no water boiling conditions inside the cooling system, an iterative approach has been adopted. At each iteration, for a fixed mass flow rate, a simple global energy balance is employed to calculate the bulk water temperature at the outlet manifold T_0 and thus the saturation pressure $P_{\text{sat}}(T_0)$. The pressure within the outlet manifold P_0 is then calculated, by means of Henry's flashing model [9], and the critical pressure at the exit section is determined as well. Subsequently, a detailed thermo-fluid-dynamic analysis is conducted to distribute the mass flow rate among the pipes, to estimate the wet wall maximum temperature, and eventually to check the no-boiling constraint. The resulting mass flow rate needed to remove the external heat load is $\dot{m} = 0.47$ kg/s.

This result has been confirmed by unsteady numerical simulations of the system startup carried out by means of the RELAP5-3D code. The relatively rapid attaining of the steady conditions is very closely confirmed. In particular, the results show that the steady value of the mass flow rate is equal to 0.47 kg/s, that is, the very same value predicted by the steady model is uncovered to within a high accuracy. In particular, it is confirmed that water does not flash within the pipe and the pressure at the pipe exit practically equals the equilibrium pressure evaluated at the stagnation temperature. The validity of the more simplified steady model of the critical discharge due to Celata et al. [14] is verified accordingly.

A discussion has been also reported about the practical implementation of the proposed active cooling system. In fact, for the reentry flow conditions considered in the present paper, a mass of water of more than 800 kg should be transported onboard and the solution could be not realistic, as storage tank and plumbing require additional mass that must fly with the vehicle. On the other hand, the advantage of the active cooling system over the other systems is unique in terms of reusability. In addition, one has to consider that the calculations made in the paper are very safe, because the thermal load

has been overestimated and the no-boiling constraint has also been imposed everywhere as an upper bound for the wet wall temperature.

As a final comment, it has to be stressed that the present paper does not represent a definite design of a new thermal protection system, but rather a detailed quantitative investigation to compare advantages and disadvantages of an innovative idea.

Acknowledgments

The paper has been carried out under contract of Thales Alenia Space (Turin) within the space program Advanced Structural Assembly, supported by the Italian Space Agency. The authors wish to thank Franco Fossati, Savino De Palo, and Giovanni Gambacciani of Thales Alenia Space for the essential technical support and helpful discussions while performing the work. The authors are strongly indebted to Idaho National Engineering and Environmental Laboratory for a free educational licensing agreement of the RELAP5-3D code, by means of which the numerical simulations have been performed. The code is copyrighted and has been secured from transfer to third parties.

References

[1] De Palo, S., and Tavera, S., "Development of the Actively Cooled Wing Leading Edge for the ASA Experiment," *37th International Conference on Environmental Systems*, Society of Automotive Engineers Paper 07-01-3201, 2007.

[2] Pinhasi, G. A., Ullmann, A., and Dayan, A., "Modeling of Flashing Two-Phase Flow," *Reviews in Chemical Engineering*, Vol. 21, Nos. 3–4, 2005, pp. 133–264.

[3] Ivashnyov, O. E., Ivashneva, M. N., and Smirnov, N. N., "Slow Waves of Boiling Under Hot Water Depressurization," *Journal of Fluid Mechanics*, Vol. 413, June 2000, pp. 149–180. doi:10.1017/S0022112000008417

[4] Nigmatulin, B. I., and Soplenkov, K. I., "Study of an Unsteady Efflux of Boiling Liquid from Channels in a Thermodynamic Non-Equilibrium Approximation," *Teplofizika Vysokikh Temperatur*, Vol. 18, 1980, pp. 118–131.

[5] Fairuzov, Y. V., "Numerical Solution for Blowdown of Pipeline Containing Flashing Liquid," *AIChE Journal*, Vol. 44, No. 9, 1998, pp. 2124–2128. doi:10.1002/aic.690440919

[6] Hahne, E., and Barthau, G., "Evaporation Waves in Flashing Processes," *International Journal of Multiphase Flow*, Vol. 26, No. 4, 2000, pp. 531–547. doi:10.1016/S0301-9322(99)00031-2

[7] Pinhasi, G. A., Dayan, A., and Ullmann, A., "Numerical Model for Bubbles Break-Up During Blowdown," AIAA Paper 2005–383, 2005.

[8] Duan, R. Q., Jiang, S. Y., Koshizuka, S., Oka, Y., and Yamaguchi, A., "Direct Simulation of Flashing Liquid Jets Using the MPS Method," *International Journal of Heat and Mass Transfer*, Vol. 49, Nos. 1–2, 2006, pp. 402–405. doi:10.1016/j.ijheatmasstransfer.2005.06.038

[9] Henry, R. E., "Two-Phase Critical Discharge of Initially Saturated or Subcooled Liquid," *Nuclear Science and Engineering*, Vol. 41, 1970, pp. 336–342.

[10] Henry, R. E., and Fauske, H. K., "Two-Phase Critical Flow of One-Component Mixtures in Nozzles, Orifices, and Short Tubes," *Transactions of the ASME, Journal of Heat Transfer*, Vol. 93, May 1971, pp. 179–187.

[11] Fraser, D. W. H., and Abdelmessih, A. H., "Study of the Effects of the Location of Flashing Inception on Maximum and Minimum Critical Two-Phases Flow Rates: Part 1, Experimental," *Nuclear Engineering and Design*, Vol. 211, No. 1, 2002, pp. 1–11. doi:10.1016/S0029-5493(01)00409-5

[12] Fraser, D. W. H., and Abdelmessih, A. H., "Study of the Effects of the Location of Flashing Inception on Maximum and Minimum Critical Two-Phases Flow Rates, Part 2, Analysis and Modelling," *Nuclear Engineering and Design*, Vol. 213, No. 1, 2002, pp. 11–30. doi:10.1016/S0029-5493(01)00410-1

[13] Simões-Moreira, J. R., and Bullard, C. W., "Pressure Drop and Flashing Mechanisms in Refrigerant Expansion Devices," *International Journal of Refrigeration*, Vol. 26, No. 7, 2003, pp. 840–848. doi:10.1016/S0140-7007(03)00070-7

[14] Celata, C. P., Cuma, M., D'Annibale, F., and Farello, G. E., "Influence of Non-Condensible Gas on Two-Phase Critical Flow," *International Journal of Multiphase Flow*, Vol. 14, No. 2, 1988, pp. 175–187. doi:10.1016/0301-9322(88)90004-3

[15] Lenclud, J., and Venart, J. ES., "Single and Two-Phase Discharge from a Pressurized Vessel," *Revue Génerale Thermique*, Vol. 35, No. 416, 1996, pp. 503–516. doi:10.1016/S0035-3159(99)80078-6

[16] Ould Didi, M. B., Kattan, N., and Thome, J. R., "Prediction of Two-Phase Pressure Gradients of Refrigerants in Horizontal Tubes," *International Journal of Refrigeration*, Vol. 25, No. 7, 2002, pp. 935–947. doi:10.1016/S0140-7007(01)00099-8

[17] Wongwises, S., and Suchatawut, M., "Simulation for Predicting the Refrigerant Flow Characteristics Including Metastable Region in Adiabatic Capillary Tubes," *International Journal of Energy Research*, Vol. 27, No. 2, 2003, pp. 93–109. doi:10.1002/er.860

[18] Yoon, H. J., Ishii, M., and Revankar, S. T., "Chocking Flow Modelling with Mechanical Non-Equilibrium for Two-Phase Two-Component Flow," *Nuclear Engineering and Design*, Vol. 236, No. 18, 2006, pp. 1886–1901. doi:10.1016/j.nucengdes.2006.02.007

[19] White, F. M., *Viscous Fluid Flow*, 3rd ed., McGraw–Hill, New York, 2006.

[20] Haaland, S. E., Simple and Explicit Formulas for the Friction Factor in Turbulent Pipe Flow, *Journal of Fluids Engineering*, Vol. 105, March 1983, pp. 89–90.

[21] Baehr, H. D., and Stephan, K., *Heat and Mass Transfer*, Springer, Berlin, 1998.